2015 International Symposium on Information Technology Convergence

Proceedings

October 15-17, 2015

Tianjin University of Science and Technology, China

Kaide Hotel 4th Floor Room Kaixuan

Session 1-D : **Communications and Network, Internet of things**

15:00-17:30, Friday. October 16, 2015

Session Chairs: Hyo Jong Lee (Chonbuk National University, Korea)
Xiankun Zhang (Tianjin University of Science and Technology, China)

ID31. Patch Based Warps Learning for Patient Identification in Hospital
Yongbin Gao, Hyo Jong Lee

ID80. A Real-Time Photoacoustic Tomograpghy Using Linear Array Probe and Detection the Rat's Kidney Inflammation
Dong ho Shin, Moung Young Lee, Sang young Lee, Heung ki Baik, Chul Gyu Song

ID23. Analysis and Design of Conventional Wideband Branch Line Balun
Qi Wang, Hojung Kang, Seungho Jeong, Junhyung Jeong, Phirun Kim, Yongchae Jeong

ID4. A Stable Algorithm for Dynamic Shortest Path Tree Update
Xiaohua Yang, Guodong Zhao, Wenjun Shi

ID5. Fault Free Cycles of Various Lengths in K-ary N-cube with Faulty Edges
Ying Zhou, Guodong Zhao, Guiyuan Jiang, Yanhui Luo

ID6. SIC-MMSE Detector with Universal Matrix Inversion
Fabrice Claude Kamaha Ngayahala, Saleem Ahmed, Sooyoung Kim

Analysis and Design of Conventional Wideband Branch Line Balun

Qi Wang, Hojung Kang, Seungho Jeong, Junhyung Jeong, Phirun Kim, and Yongchae Jeong

Division of Electronics and Information Engineering
Chonbuk National University
Jeonju-Si, Republic of Korea
ycjeong@jbnu.ac.kr

***Abstract*—This paper presents a design and analysis of wideband branch line balun. Theoretical analysis shows that the wideband return loss characteristic of proposed circuit with two transmission poles can be obtained by controlling characteristic impedance (Z_t) of horizontal transmission line. The proposed circuit has been designed at a center frequency (f_0) of 2.6 GHz. The measured results are in good agreement with the simulation results. From the measurement, the power divisions were -3.06 dB and -3.08 dB. And the return loss was 21.9 dB at f_0 and better than 20 dB over bandwidth of 0.98 GHz (2 GHz-2.98 GHz). The phase difference between two balance ports is 180 ± 5º in frequency range of 1.98 GHz to 2.98 GHz.**

Keywords- Coupled line, even- and odd-modes, wideband branch-line balun, wideband impedance transformer.

I. Introduction

Balun is a three-port network which is used to transform unbalanced input signal into two balanced output signals and vice versa. The various types of balun have been reported such as Marchand balun, branch line balun, and coplanar-waveguide balun [1-11]. Marchand balun is composed of two sets of coupled transmission-line sections that it can provided 180º phase difference between two balanced ports [1-3].

Recently, the 3-port baluns consisting of symmetrical 4-port branch line network with terminating one as open circuited were reported in [4-7]. In [6], a branch line balun with stubs on vertical branches, which can eliminate unwanted even-mode signal and reduce circuit size, was presented. However, the circuit performances have relatively narrow bandwidth. On the other hand, the bandwidth enhancement of branch line balun due to attaching a short-circuited quarter-wavelength stub to the output junction port was described in [7]. Similarly, a wideband balun using the coupled line section and a defected ground structure (DGS) was presented in [8]. Similarly, the wideband balun using artificial fractal shaped composite right/left handed transmission lines (CRLH TL) was reported in [9].

In this paper, a new wideband branch line balun is presented by choosing different characteristic impedances of horizontal and vertical lines in the branch structure. To validate the design equations of the proposed branch line balun, a microstrip balun with equal termination impedance are design, simulated, and measured at a design center frequency (f_0) of 2.6 GHz.

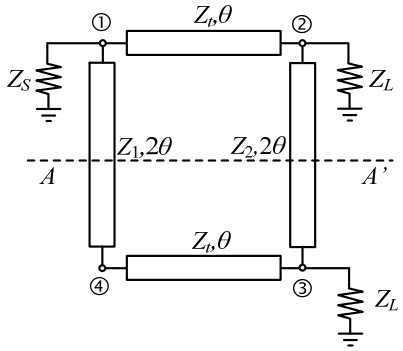

Fig. 1. Proposed structure of wideband branch line balun.

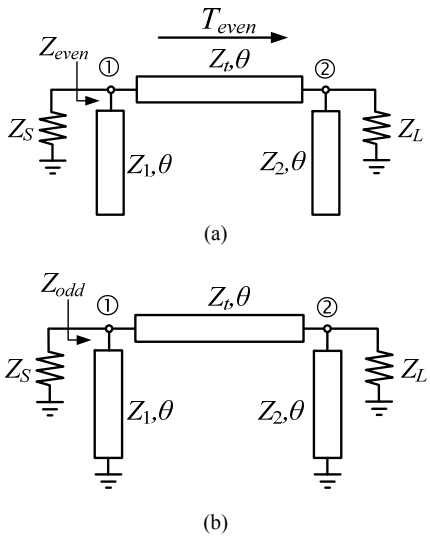

Fig. 2. Equivalent circuits of proposed wideband branch line balun: (a) even-mode and (b) odd-mode excitations.

II. Circuit Design

Fig. 1 shows the proposed structures of wideband branch line baluns. The proposed circuit consist of a pair of horizontal quarter wavelength ($\lambda/4$) transmission lines with a characteristic impedance Z_t and a pair of vertical half wavelength ($\lambda/2$) transmission line with characteristic impedance Z_1 and Z_2 (assumed $\theta = \pi/2$ at f_0). Because the proposed structure is composed of a symmetrical four-ports network in which one of the ports is terminated as an open circuit, the even- and odd-mode analysis can be applied [4] for design and analysis. In order to operate the proposed circuit as

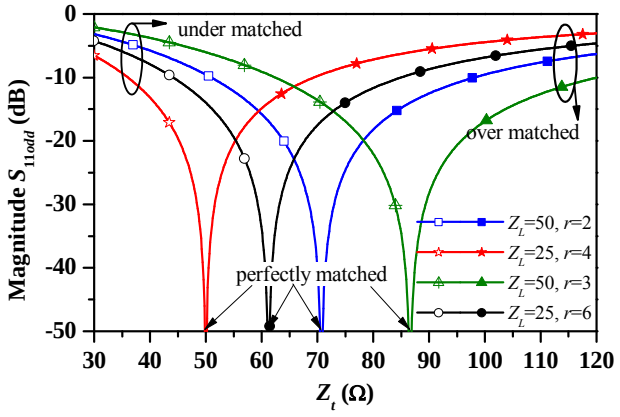

Fig. 3. The return loss characteristics at center frequency (f=f_0) according to Z_t with Z_L = 50 Ω, 25 Ω and r = 2, 3, 4, 6.

balun, the following conditions should be maintained which are given as (1).

$$T_{even} = 0 \tag{1a}$$

$$Z_{even} + Z_{odd} = 2Z_s, \tag{1b}$$

where T_{even}, Z_{even}, Z_{odd}, and Z_s are transmission coefficient, even- and odd-mode impedances, and source impedance, respectively. Specially, (1a) shows that to achieve perfect amplitude and phase balance, the balun has to prevent a transmission stop in the even-mode excitation. In addition, (1b) shows that the sum of the even- and odd-mode impedances must be twice of the source impedance in order to get perfect matching condition at balun input port.

To meet the balun conditions in (1), the even- and odd-mode excitations are applied to the proposed circuit. The equivalent circuits of two modes are shown in Fig. 2. Under the even-mode excitation, the symmetrical plane of AA' can be considered as a perfect magnetic wall (open-circuited). Therefore, the $\lambda/2$ transmission lines are split in half along the center line with the open-circuited shown in Fig. 2(a). These two open stubs with $\lambda/4$ transmission line will transform open-circuited impedance into short-circuited (Z_{even} = 0) at the connected points and can provide the transmission coefficient (T_{even} = 0) at f_0, which satisfies condition (1a). Under the odd-mode excitation, the $\lambda/2$ transmission lines are split in half along the center line with the short-circuited as shown in Fig. 2(b). Under this excitation, (1b) reduces to (2) with the condition of Z_{even} = 0.

$$Z_{odd} = 2Z_s \tag{2}$$

From (2), the input impedance of equivalent odd-mode circuit should be designed to match with $2Z_s$.

From the odd-mode excitation, the return loss (S_{11odd}) and insertion loss (S_{21odd}) are given as (3) from overall *ABCD*-parameters.

$$S_{11odd} = \frac{Z_L A_{odd} + B_{odd} - rZ_L^2 C_{odd} - D_{odd} rZ_L}{Z_L A_{odd} + B_{odd} + rZ_L^2 C_{odd} + D_{odd} rZ_L} \tag{3a}$$

$$S_{21odd} = \frac{2Z_L\sqrt{r}}{Z_L A_{odd} + B_{odd} + C_{odd} rZ_L^2 + D_{odd} rZ_L} \tag{3b}$$

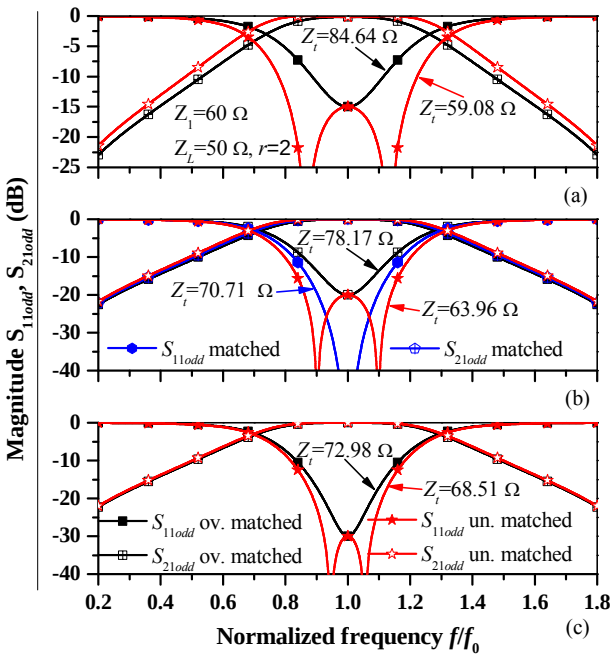

Fig. 4. Reflection and transmission characteristics with different matched conditions for: (a) S_{11odd} = -15 dB, (b) S_{11odd} = -20 dB, and (c) S_{11odd} = -30 dB.

$$A_{odd} = \cos\theta + \frac{Z_t \sin\theta}{Z_2 \tan\theta} \tag{3c}$$

$$B_{odd} = jZ_t \sin\theta \tag{3d}$$

$$C_{odd} = j\left(\frac{\sin\theta}{Z_t} - \frac{\cos\theta}{Z_2\tan\theta} - \frac{Z_t\sin\theta}{Z_1 Z_2 \tan^2\theta} - \frac{\cos\theta}{Z_1\tan\theta}\right) \tag{3e}$$

$$D_{odd} = \cos\theta + \frac{Z_t \sin\theta}{Z_1 \tan\theta}, \qquad r = \frac{Z_S}{Z_L} \tag{3f}$$

$$\theta = \frac{\pi}{2}\frac{f}{f_0}, \tag{3g}$$

where Z_S, Z_L, and r are the source impedance, load impedance, and impedance transforming ratio between source and load impedances, respectively. The return loss of odd-mode equivalent circuit at f_0 can be reduced to (4).

$$S_{11odd}\big|_{f=f_0} = \frac{Z_t^2 - rZ_L^2}{Z_t^2 + rZ_L^2} \tag{4}$$

From (4), the return loss at f_0 only depends on Z_t, and are independent of Z_1 and Z_2. Therefore, the return loss can be controlled by only Z_t. Fig. 3 shows the return loss characteristic versus Z_t with Z_L = 50 Ω, 25 Ω and r = 2, 3, 4, 6, respectively. From this figure, there are three different matched regions depending on value of Z_t which can be described as (5).

$$Z_t < Z_L\sqrt{r} \quad : \text{under-matched} \tag{5a}$$

$$Z_t = Z_L\sqrt{r} \quad : \text{perfectly matched} \tag{5b}$$

$$Z_t > Z_L\sqrt{r} \quad : \text{over-matched} \tag{5c}$$

Therefore, Z_t with the specified return loss can be found as (6) for the under-matched region.

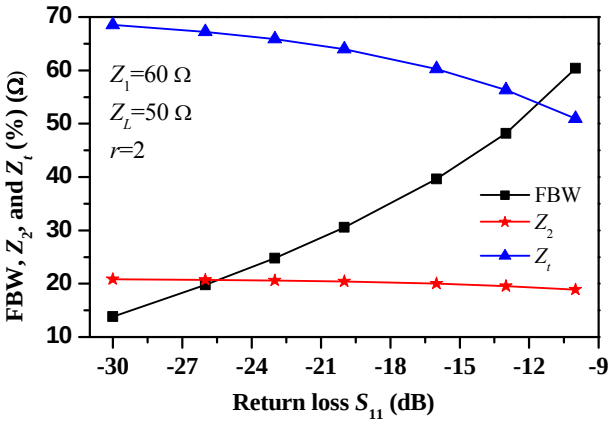

Fig. 5. Design graph of balun according to return loss (S_{11}) characteristics.

$$Z_t = Z_L\sqrt{\frac{r\left(1-S_{11odd}\big|_{f=f_0}\right)}{1+S_{11odd}\big|_{f=f_0}}} \tag{6}$$

Similarly, Z_t with the specified return loss can be found as (7) for the over-matched region.

$$Z_t = Z_L\sqrt{\frac{r\left(1+S_{11odd}\big|_{f=f_0}\right)}{1-S_{11odd}\big|_{f=f_0}}} \tag{7}$$

In the perfectly matched region, S_{11odd} becomes zero so that Z_t is related with Z_L and r as (8).

$$Z_t = Z_L\sqrt{r} \tag{8}$$

After obtaining Z_t, the relation between Z_2 and Z_1 can be found as (9), which can provide two poles in the passband.

$$Z_2 = \frac{Z_t Z_1}{rZ_t + rZ_1 - Z_1} \tag{9}$$

Fig. 4 shows the graph of reflection and transmission characteristics for the specified return losses of 15 dB, 20 dB, and 30 dB at f_0. As seen from this graph, two poles are obtained only in case of the under-matched region. However, there is only one pole in case of the perfectly and over-matched regions. Therefore, the under-matched region is preferable because of two poles in return loss characteristic, which provide the sharp and wideband characteristics.

The locations of poles in the under-matched region can be derived from (3a) as (10).

$$f_{p1,p2}/f_0 = 1\mp\left[1-\frac{2}{\pi}\tan^{-1}\sqrt{\frac{rZ_L^2Z_t\left(Z_1+Z_t+Z_2\right)}{Z_1Z_2\left(rZ_L^2-Z_t^2\right)}}\right] \tag{10}$$

Fig. 5 shows a design graph in case of the under-matched region of the odd-mode excitation. This figure investigate the relation between Z_1, Z_2, Z_t, and FBWs, with different values of the return loss. As seem from this figure, the decrease of the return loss causes the increase of the bandwidth and the small decrease of the characteristic impedance Z_2. Moreover, the characteristic impedance of Z_t is decreased with the decrease of the return loss.

In order to verify the design analysis of the proposed structure, the balun with the return loss of 20 dB was simulated at f_0 of 2.6 GHz. In this simulation, all three ports are

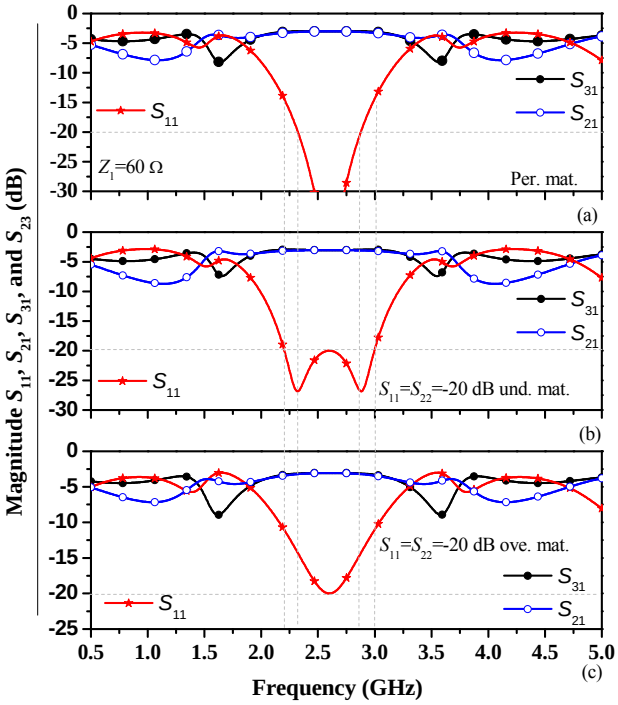

Fig. 6. S-parameter characteristic of wideband balun.

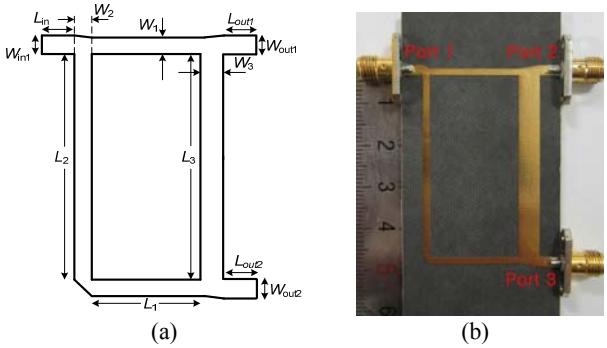

Fig. 7. (a) EM simulation layout and (b) physical dimensions of the proposed balun.

terminated with 50 Ω which requires r = 2 according to (2). Therefore, the extracted values of Z_t according the design specifications are 63.96 Ω, 70.71 Ω, and 78.17 Ω for the under-, perfectly, and over-matched regions, respectively. The value of Z_1 was chosen as 60 Ω and Z_2 can be calculated using (9). Fig. 6 shows the simulation results of proposed balun which exactly satisfies design specifications. Moreover, the bandwidth of under-matched regions is wider and sharper than the perfectly and over-matched regions with two transmission poles in the passband.

III. Simulation and Measurement

For experimental validation of proposed structure, the wideband balun was designed at f_0 of 2.6 GHz. The designed return loss was 20 dB at f_0. From above analysis, the under-matched region was chosen for the wideband characteristic. The circuits was fabricated on a substrate RT/Duroid 5880 with dielectric constant (ε_r) of 2.2 and thickness (h) of 31 mils. The electromagnetic (EM) simulation was performed using HFSS v15 of ansoft.

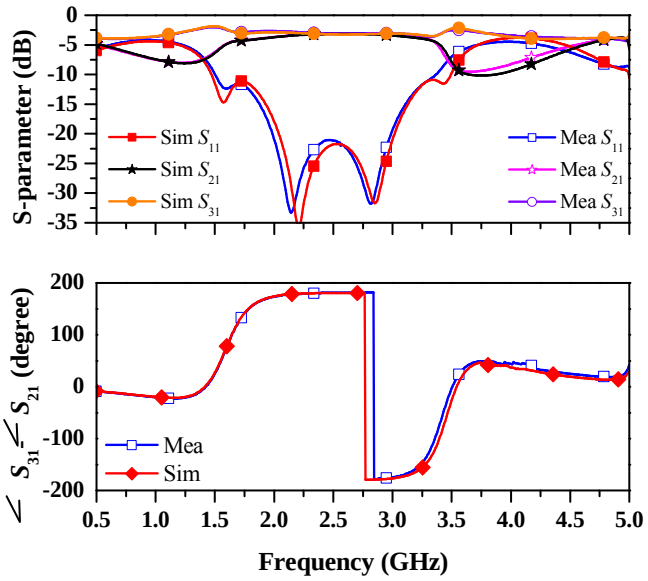

Fig. 8. EM simulation and measurement results.

TABLE I
PHYSICAL DIMENSIONS OF THE PROPOSED WIDEBAND BALUN

W_1=1.54 mm	L_1=21 mm	W_2=2.4 mm	L_{in}=5 mm
W_2=1.57 mm	L_2=42.5 mm	W_{out1}=2.4 mm	L_{out1}=5 mm
W_3=5 mm	L_3=42.5 mm	W_{out2}=2.4 mm	L_{out2}=5 mm

From (6), Z_t = 63.96 Ω for the under-matched region was calculated to meet the return loss of 20 dB in case of Z_L = 50 Ω and r = 2. With Z_1 = 60 Ω, Z_2 = 20.42 Ω was calculated by using (9). Fig. 7 shows the EM simulation layout and a photograph of the fabricated wideband balun with the circuit size of 37 × 55 mm^2. The physical parameters of this circuit are given in Table I after a slight optimization. Fig. 8 shows the EM simulation and measurement results of wideband balun. The measured results are good agreement with the simulation restuls. From the measurement, the magnitudes of S_{21} and S_{31} are obtained as -3.06 dB and -3.08 dB at f_0. The amplitude imbalance of -3 ± 0.6 dB was obtained within the bandwidth 0.98 GHz (2 - 2.98 GHz). The return loss (S_{11}) is better than 20 dB over the bandwidth 0.98 GHz (2 - 2.98 GHz). The measured phase deviation between two output ports is 180 ± 5^o within 38.46% of FBW (1.98 - 2.98 GHz).

IV. Conclusion

In this paper, a design of wideband balun using single section branch line structure was proposed. There were three different matching regions had been categorized according to the return loss characteristics. The wideband characteristics was obtained with the under-matched region. The theoretical and measurement results were provided for the validation. The measurement results have a good agreement with the simulation results. The proposed structure is simple to design and fabricate, so that expected to applicable for the wideband RF systems.

References

[1] C. Shie, Y. Pan, K. Sheng, and Y. Chiang, "A miniaturized microstrip balun constructed with two λ/8 coupled lines and a redundant line," *IEEE Microw. Wireless Compon. Lett.*, vol. 20, no. 12, pp. 663–665, Dec. 2010.

[2] K. Ang and I. Robertson, "Analysis and design of impedance-transforming planar marchand baluns," *IEEE Trans. Microw. Theory Techn.*, vol. 49, no. 2, pp. 402-406, Feb. 2012.

[3] C. Tseng and Y. Hsiao, "A new broadband marchand balun using slot-coupled microstrip lines," *IEEE Microw. Wireless Compon. Lett.*, vol. 20, no. 3, pp. 157-159, Mar. 2010.

[4] Y. Leong, K. Ang, and C. Lee, "A derivation of a class of 3-port baluns from symmetrical 4-port networks," *IEEE Internat. Microw. Sympos. Digest*, pp. 1165-1168, 2002.

[5] H. Zhan and H. Xin, "Dual-band branch-line balun for millineter-wave applications," *IEEE Internat. Microw. Sympos. Digest,* pp. 717-720, 2009.

[6] M. Park and B. Lee, "Stubbed branch line balu," *IEEE Microw. Wireless Compon. Lett.*, vol. 17, no. 3, pp. 169-171, Mar. 2007.

[7] J. Li, S. Qu, and Q. Xue, "Miniaturised branch-line balun with bandwidth enhancement," *Electron. Lett.*, vol. 43, no. 17, pp. 931-932, Aug. 2007.

[8] B. Li, X. Wu, J. Yang, and W. Wu, "A defected-ground coupled line section with two shorts for wideband balun application," *Asia Pacific Microw. Conf.*, pp. 2030-2032, 2009.

[9] H. Xu, G. Wang, X. Chen, and T. Li, "Broadband balun using fully artificial fractal-shaped composite right/left handed transmission line," *IEEE Microw. Wireless Compon. Lett.* vol. 22, no. 1, pp. 16-18, Jan. 2012.

[10] V. Velidi, A. Pal, and S. Sanyal, "Harmonics and size reduced microstrip branch-line baluns using shunt open-stubs," *Internation. Jour. RF Microw. Computer-Aided Engineering,* vol 21, no. 2, pp. 199-205, Mar. 2011.

[11] J. Lim, D. Kim, Y. Jeong, and D. Ahn, "A size-reduced CPW balun using a "X"-crossing structure," *European Microw. Conf.*, pp. 521-524, 2005.